

NOTICE WARNING CONCERNING COPYRIGHT RESTRICTIONS:
The copyright law of the United States (title 17, U.S. Code) governs the making of photocopies or other reproductions of copyrighted material. Any copying of this document without permission of its author may be prohibited by law.

COMPUTER ANALYSIS OF NEURONAL STRUCTURE¹

by

D.R. Reddy, W.J. Davis², R.B. Ohlander, and D.J. Bihary
Computer Science Department
Carnegie-Mellon University
Pittsburgh, Pa.

FEB 1 1973

¹This research is principally supported by the National Science Foundation under contract no. GJ32784 and in part by NIH Grant NS-09050.

²Permanent address: The Thimann Laboratories, University of California, Santa Cruz, California.

TABLE OF CONTENTS

I. INTRODUCTION

- A. Purpose
- B. Background
- C. Current Methods of Analysis
- D. The Need for Quantification

II. THE SYNAPS SYSTEM

- A. Overview of the System
- B. The Research Computer System (Hardware)
 - 1. Input Devices
 - 2. Output Devices
- C. The Programming System (Software)
 - 1. Digitization and Analysis of Sections
 - a. The Manual Method
 - b. The Automatic Method
 - 2. Generation of the Three-Dimensional Model
 - a. Alignment of Sections
 - b. Assembly of Sections
 - 3. Graphic Display of the Model
 - 4. Analysis of Reconstructed Neurons
 - a. Qualitative Studies
 - b. Quantitative Studies

III. SUMMARY AND CONCLUSIONS

INTRODUCTION

A. PURPOSE

A fundamental goal of neuroscientists is to correlate neuronal morphology with neuronal function, both at the level of single nerve cells and that of neuronal networks. This goal has seldom been obtained to a satisfactory degree, partially because quantitative methods for describing neuronal structure are lacking. In this paper we will describe a computer-based system, SYNAPS (Symbolic Neuronal Analysis Programming System), which is being developed at Carnegie-Mellon University for the reconstruction and analysis of nerve cells and networks. In particular, we will describe programs that perform data gathering, analysis, generation and representation of three-dimensional models,* display of the models from various viewing angles, and analysis of neural structure.

B. BACKGROUND

All of the complex integrative operations of the nervous system result more or less directly from neuronal structure, i.e., from the geometrical characteristics of single neurons and from the patterns of interconnection between them. On the cellular level, the integrative capacities of single nerve cells are closely related to geometrical features such as size (Henneman (1957); Henneman *et al.* (1965); Davis (1971); Hinkle and Camhi (1972)), the detailed shape of individual dendrites (which helps to determine the space constant) and the proximity of synapses to integrative regions such as spike-initiating zones (Rall (1967); Rall *et al.* (1967); Rall and Shepherd (1968)). Important integrative properties of neurons may even depend upon the gross morphology of dendritic fields (Ramón-Moliner (1962, 1968); Globus and Sheibel (1967); Munagai (1967)). In frog retinal ganglion cells, for example, the shapes of dendritic trees appear to represent the code for the detection of specific visual shapes (Pomeranz and Chung (1970)). Indeed, the highly characteristic shapes of many nerve cells, as expressed by their diagnostic common names (stellate cells, basket cells, mossy fibers, etc.), may signify that the gross anatomy of dendritic fields is of general integrative significance.

On the population level, it is likely that the relative spatial positions of neurons is an important and in some cases major determinant of the integrative properties of the population. One can imagine, for example, neurons responding sequentially to a traveling wave of neuronal activity and/or performing crucial spatio-temporal transformations on the basis of relative position in the neuronal matrix which supports the wave (Beurle (1956); Verzeano and Negishi (1960); Verzeano (1963); Globus and Sheibel (1967)). Such an arrangement could contribute to the production of stereotyped motor output programs (Davis (1969)). Indeed, in the cat cerebellum, Purkinje cells are regularly spaced along "beams" of presynaptic parallel fibers. As a result of this spatial arrangement, Purkinje cells fire in a stereotyped temporal sequence in response to electrical or natural stimulation of afferent pathways (Fox and Barnard (1957); Freeman (1969)).

*The word "model" throughout this paper means a computer-generated representation of a tangible, physical structure, and not a theory as in the case of models of behavior.

Finally, none of the structural parameters discussed above are static. Instead, the structure of the nervous system is in a constant state of flux, as a result of natural, genetically-regulated processes such as ontogeny and growth, or as a result of pathological processes such as the degeneration associated with many diseases of the nervous system. Changes in neuronal structure may even underlie the most sophisticated operations of the nervous system, including learning and other forms of neuronal plasticity (Hilgard (1964)).

C. CURRENT METHODS OF ANALYSIS

The basic approach used to study the structure of the nervous system has been unchanged for over a century. Small pieces of neuronal tissue are treated with chemicals which selectively color certain nerve cells or regions, thereby emphasizing specific features without altering the original structure significantly. This approach reached a zenith in the gifted hands of Ramon y Cajal, whose studies on the vertebrate nervous system near the beginning of this century set a standard which is still unsurpassed (Ramon y Cajal (1911)). Progress has been slower among invertebrates, at least in part because histological stains which are effective in vertebrate nervous tissue are at best capricious when applied to invertebrates. Recently a new histological technique was introduced which is applicable to invertebrate and vertebrate nervous systems alike -- that of intracellular dye injection (Thomas and Wilson (1966); Kato *et al.* (1968); Stretton and Kravitz (1968)). The occurrence of this symposium is testimony to the explosive burst of research stimulated by the introduction of this method.

The full potential of intracellular dye injection has been realized in invertebrate nervous systems, where single neurons can be reliably identified from one animal to the next. In the lobster Homarus americanus, for example, each of four segmental ganglia in the abdomen controls a pair of locomotory appendages, the swimmerets. Intracellular stimulation and recording has been utilized to map the soma positions of the motoneurons which operate a swimmeret (Davis (1971), Figs. 1 and 2). Once the position of a neuron is located in this manner, intracellular dye injection may be applied to unravel the geometry and synaptic connections of the neuron.

The details of the dye injection techniques are fully described elsewhere in this volume (Kater *et al.* (1973)). Basically they involve filling a neuron with a marker substance which remains confined within the neuron so that the central and peripheral projections of the cell may be followed in subsequent whole mounts or thin sections of the tissue. The most commonly used marker substance has been the textile dye Procion Yellow, which appears brilliant yellow when viewed with the fluorescence microscope (Fig. 3). Recently a useful new procedure has been developed, utilizing injection of cobalt chloride (Pitman *et al.* (1972); Cohen (1973)). This substance has the advantage that it is electron dense and can therefore be detected using the electron microscope.

The kind of neuronal reconstruction which can be achieved using intracellular dye injection is illustrated in figure 4 and in the pictures presented by other contributors to this volume (Cohen (1973); Murphey (1973); Kravitz (1973); Mulloney (1973); Selverston (1973)). In addition to these reconstructions of neuronal geometry, one

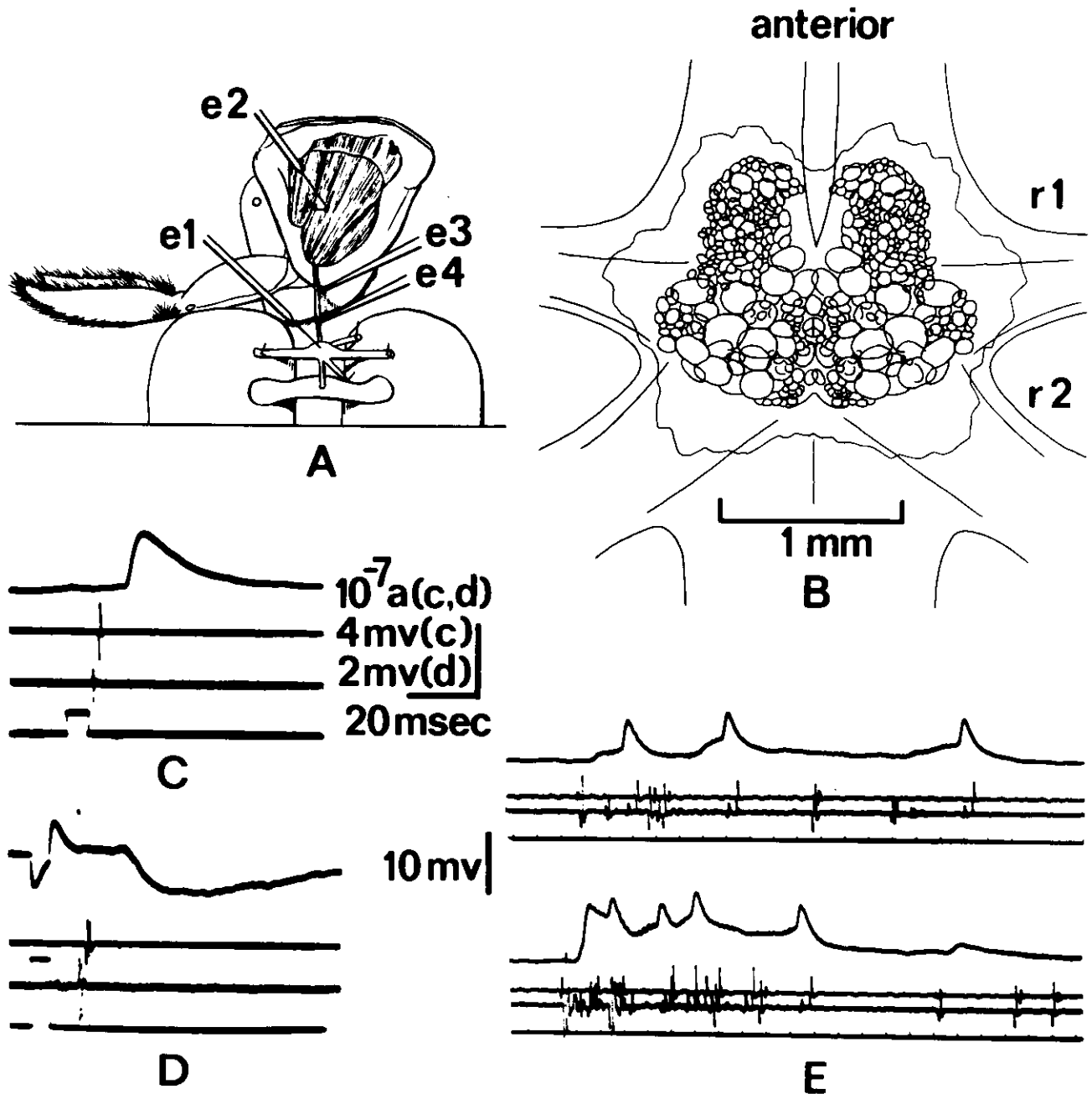


Figure 1. Identification of the cell bodies (somata) of the swimmeret motoneurons. A, the preparation, consisting of a single swimmeret, its muscles and its nerve supply (the first abdominal nerve root and the corresponding segmental abdominal ganglion). e1 and e2, intracellular microelectrodes for stimulating single motoneuron somata and recording the muscle responses, respectively. e3 and e4, suction electrodes for extracellular recording of motoneuron action potentials. B, ventral view of the desheathed abdominal ganglion, as seen at low power through a binocular microscope. Numerous nerve cell bodies are visible. C and D, intracellular records of an excitatory (upper trace in C) and inhibitory (upper trace in D) junctional potential in the main power-stroke muscle, caused by stimulating identified somata (lower trace on each record) while recording the corresponding action potentials (middle two traces in each record). E, simultaneous intracellular/extracellular recordings from an identified motoneuron. From Davis (1971).

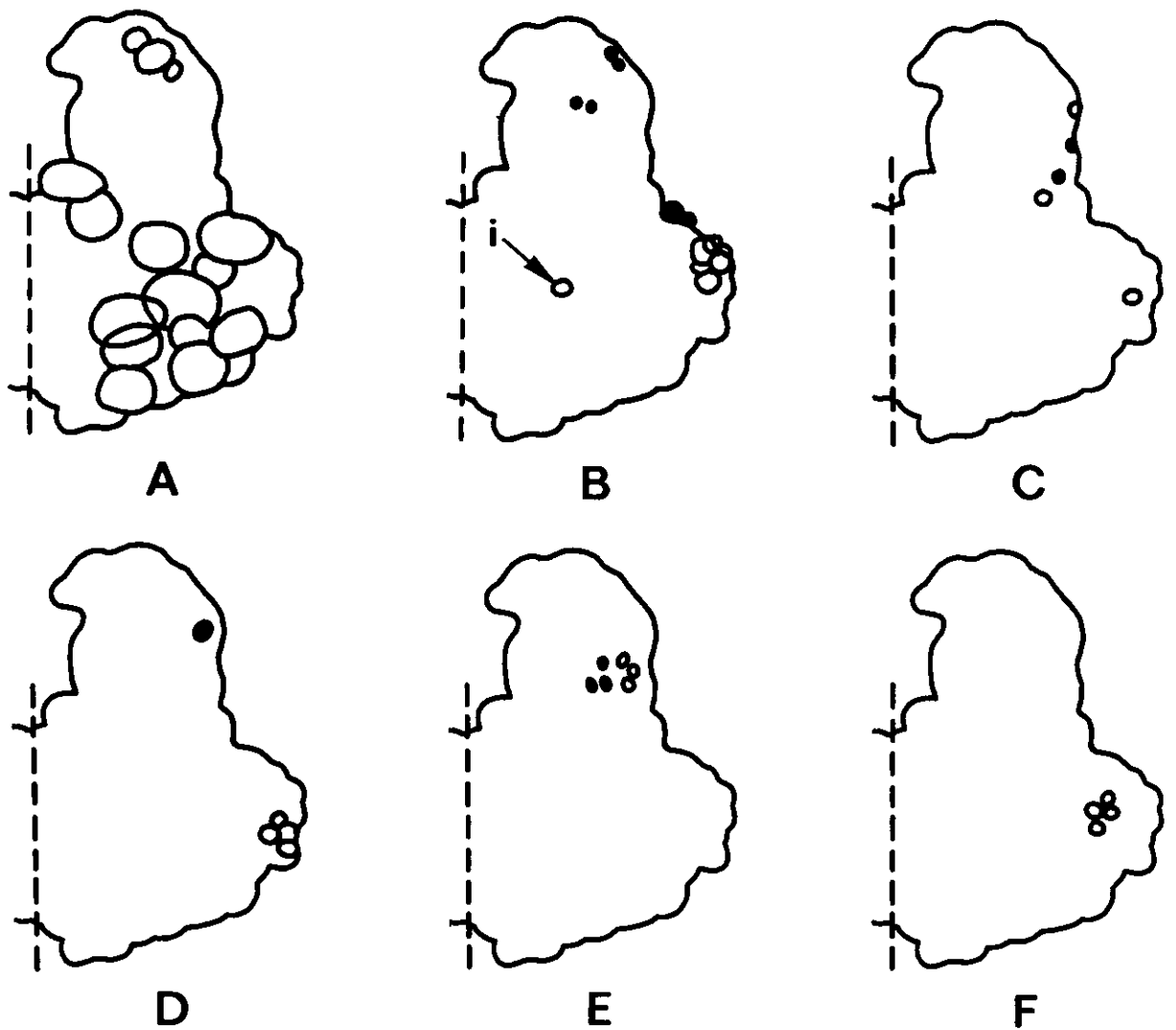


Figure 2. Soma maps of the left half of the third abdominal ganglion, seen in ventral aspect. A, somata of flexor and extensor motoneurons (from Otsuka *et al.* (1967)). B-F, swimmeret motoneuron somata. B: ○, somata of motoneurons to the main powerstroke muscle; ●, main return-stroke muscle. i, common powerstroke inhibitor. C: ○, abductor muscle of the exopodite; ●, adductor of exopodite. D: ○, rearward powerstroke muscle; ●, pronator of endopodite. E: ○, curler of exopodite; ●, curler of endopodite. F, accessory powerstroke muscle. From Davis (1971).



Figure 3. High power fluorescence photomicrograph of a section containing branches of a power stroke swimmeret motoneuron which has been injected with the dye Procion Yellow.

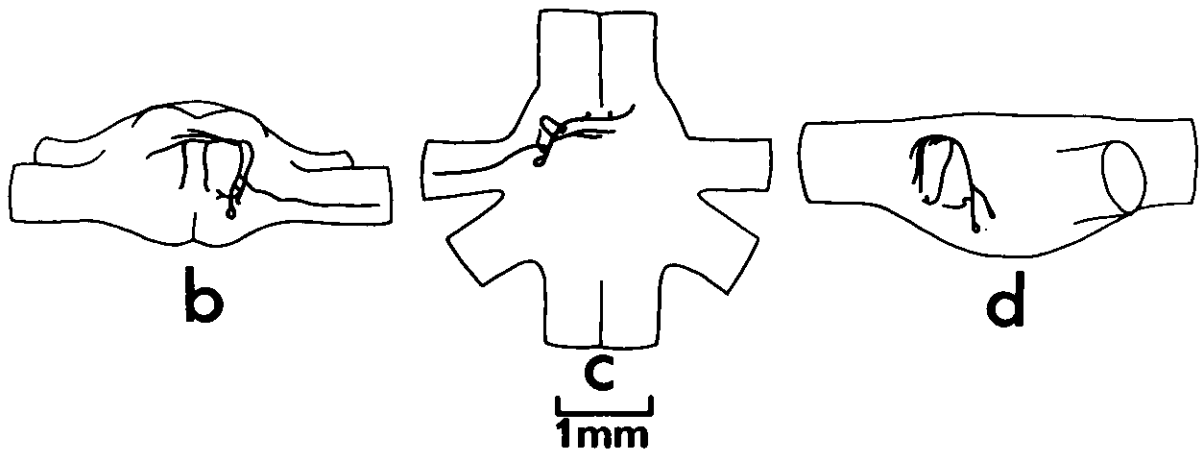


Figure 4. Reconstruction of the third abdominal ganglion and a single powerstroke motoneuron within it, as seen from the anterior. This cell is the same as shown in figure 3. A, three-dimensional drawing. B-D, estimated planar projections of the injected neuron. Anterior is toward the top and left in C and D, respectively. From Davis (1970).

can follow the fine branches of the dendrites of injected neurons to their terminals, which are commonly tightly apposed to the branches of other neurons (Fig. 3; Fig. 5). Circumstantial evidence suggests that such connections are functional synapses. In the crayfish abdomen, for example, certain flexor motoneurons can be excited by stimulating the heterolateral but not the homolateral giant fibers. Injection of these same motoneurons has shown independently that they make close contact with heterolateral but not homolateral giant fibers (Kennedy *et al.* (1969)). In the lobster swimmeret system, a cross-sectional map of all neurons which made contact with a single injected motoneuron has been constructed (Fig. 6A), and this map is similar to a cross-sectional map of neurons which are known independently to excite the swimmeret motoneurons (Fig. 6B). Thus, the intracellular dye injection method can be used to determine the geometry of individual nerve cells, and -- subject to direct confirmation with the electron microscope -- their pattern of interconnection with other nerve cells.

D. THE NEED FOR QUANTIFICATION

Reconstructions of ganglia achieved to date (Fig. 4) are esthetically pleasing, and they have provided new information on neuronal geometry. Their utility, however, is severely limited by the lack of precision and the absence of quantification. How many microns in diameter are individual dendrites? How rapidly do dendrites taper and branch, with attendant functional implications? How do particular structural parameters (e.g. dendrite size) relate to specific functional characteristics (e.g. neuronal threshold)? What are the spatial coordinates of the dendrites relative to other neurons, and how do these relative positions relate to the output patterns of the neurons? How do structural parameters change during learning and development? Satisfactory answers to these questions cannot be obtained until precise methods for accurately describing neuronal structure are developed. In response to this need a number of investigators have begun to apply quantitative and/or computer techniques to the problem of reconstructing and describing nerve cells (Fox and Barnard (1957); Mannen (1964); Ledley (1964); Levinthal and Ware (1972); Woolsey *et al.* (1972); Selverston (1973)). In this article we describe our initial efforts toward the reconstruction and analysis of neuronal structure, utilizing the specific example of the lobster swimmeret system.

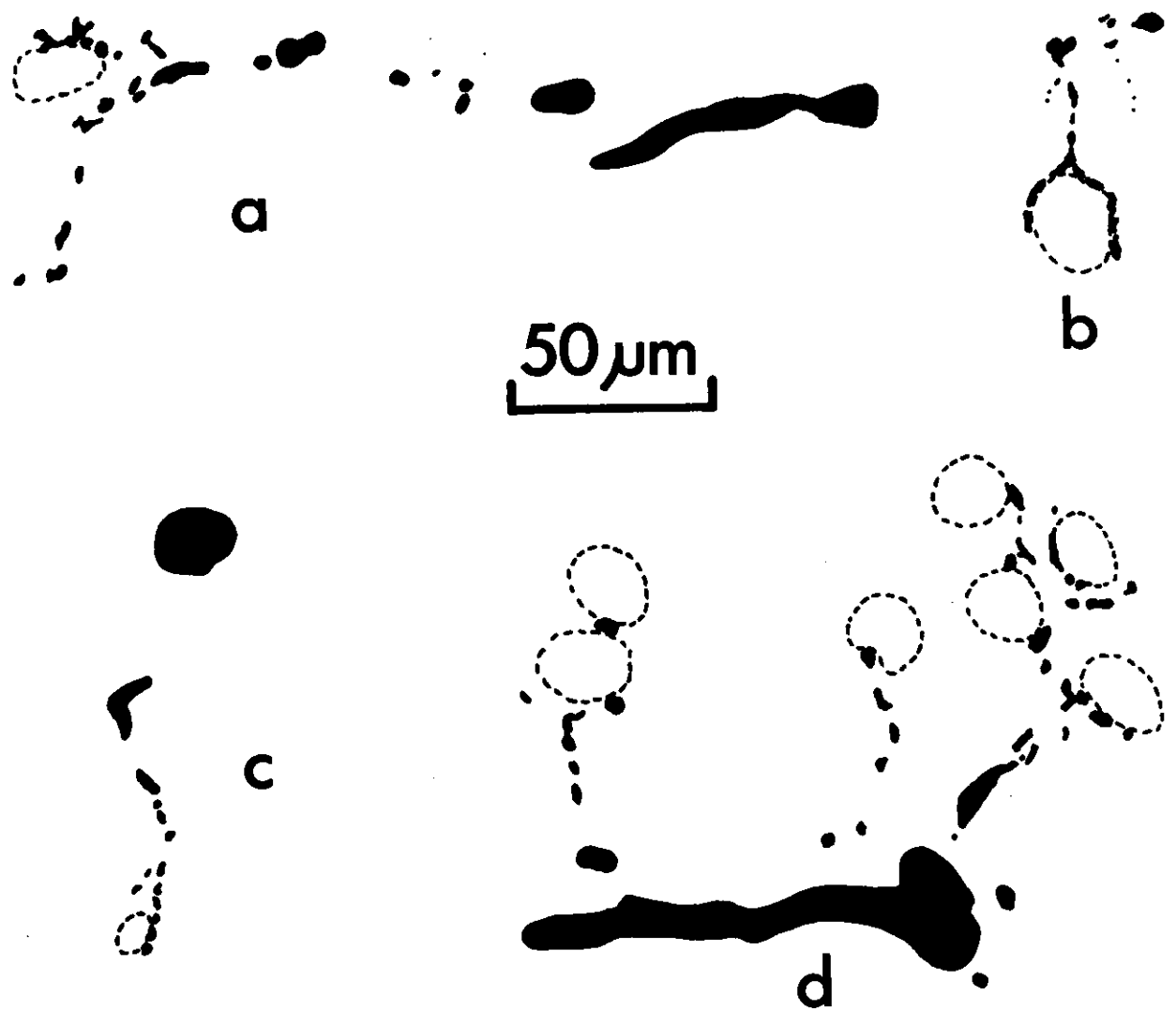


Figure 5. Typical profiles of the injected powerstroke motoneuron shown in figure 3, traced from photomicrographs such as the one shown in figure 3. B of this figure corresponds to figure 3. From Davis (1970).

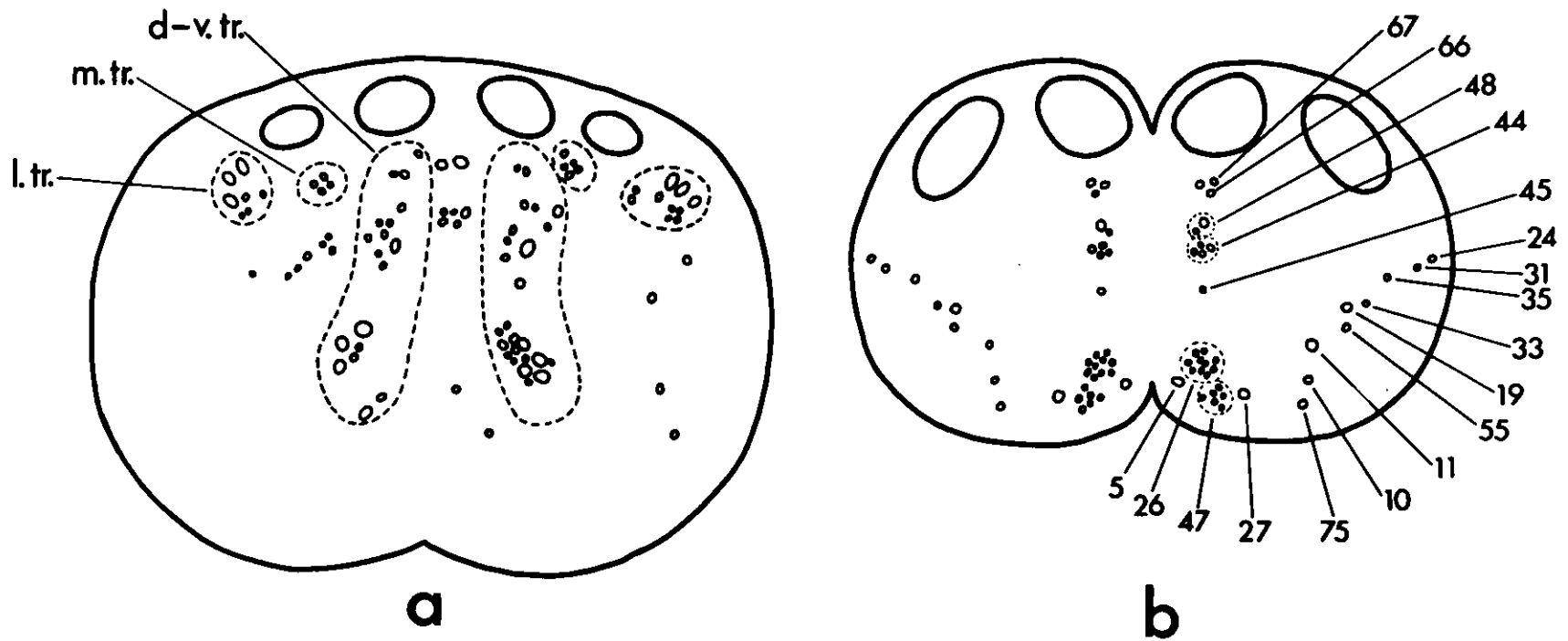


Figure 6. a, map of cross sections of all axons passing through the third abdominal ganglion which were contacted (Fig. 5) by the cell illustrated in figure 4. The axons are grouped into a bilaterally-symmetrical lateral tract (l. tr.), medial tract (m. tr.) and a dorso-ventral tract (d-v.tr.). b, map of cross section of all axons in the crayfish nerve cord which are known to have functional effects on swimmeret motoneurons (reconstructed from the data of Wiersma and Hughes (1960 and 1961)). Certain populations of axons in the "structural" map (a) are congruent with presumably homologous populations in the "functional" map(b). From Davis (1970).

THE SYNAPS SYSTEM

A. OVERVIEW OF THE SYSTEM

SYNAPS is the Symbolic Neuronal Analysis Programming System, being developed at Carnegie-Mellon University, for the three-dimensional reconstruction of dye-injected, serially-sectioned neurons on a computer. To achieve the goals implicit in our research objectives this system must satisfy several functional requirements. Specifically, it must:

1. generate digital images of the serial sections of the injected neuron and the ganglion which contains it;
2. process the digitized images to locate the boundary of the ganglion, the dendritic cross-sections of the dye-injected neuron, and other structures of interest (giant fibers);
3. align the relevant boundaries from each section with those of adjacent sections;
4. assemble all the sections of the ganglion together to generate a concise three-dimensional model of the ganglion and the relevant neurons within it;
5. display the ganglion and the injected neuron on a cathode ray tube (CRT), or other output devices, at any specified viewing angle;
6. quantitatively describe the structure of identified neurons; and
7. assemble two or more reconstructed neurons from different injection experiments into a single topological map, and perform appropriate quantitative analysis of relative spatial relationships.

The SYNAPS system is envisioned, in its final version, as meeting the above requirements in four operations (Fig. 7A): image digitization and processing of information from serial sections, generation of a three dimensional model from these data, display of the model from any desired viewing angle, and quantitative analysis and comparison of neuronal structures. The system is highly interactive, i.e., the computer operations are performed in close symbiosis with the researcher. In this fashion, subjective judgements can be introduced -- a feature we believe essential in dealing with data from intracellular dye injection (Kater *et al.* (1973)).

B. THE RESEARCH COMPUTER SYSTEM (HARDWARE)

A computer system capable of performing the above operations must be a large scale, on-line interactive system with several special purpose devices. It must be large scale in order to handle the vast amounts of raw data and extensive processing. It must be an interactive system to allow close supervision by the researcher. In addition, the system must have facilities for input of image data and for visual display of neural structures. The computer system we are presently using (Fig. 7B) consists

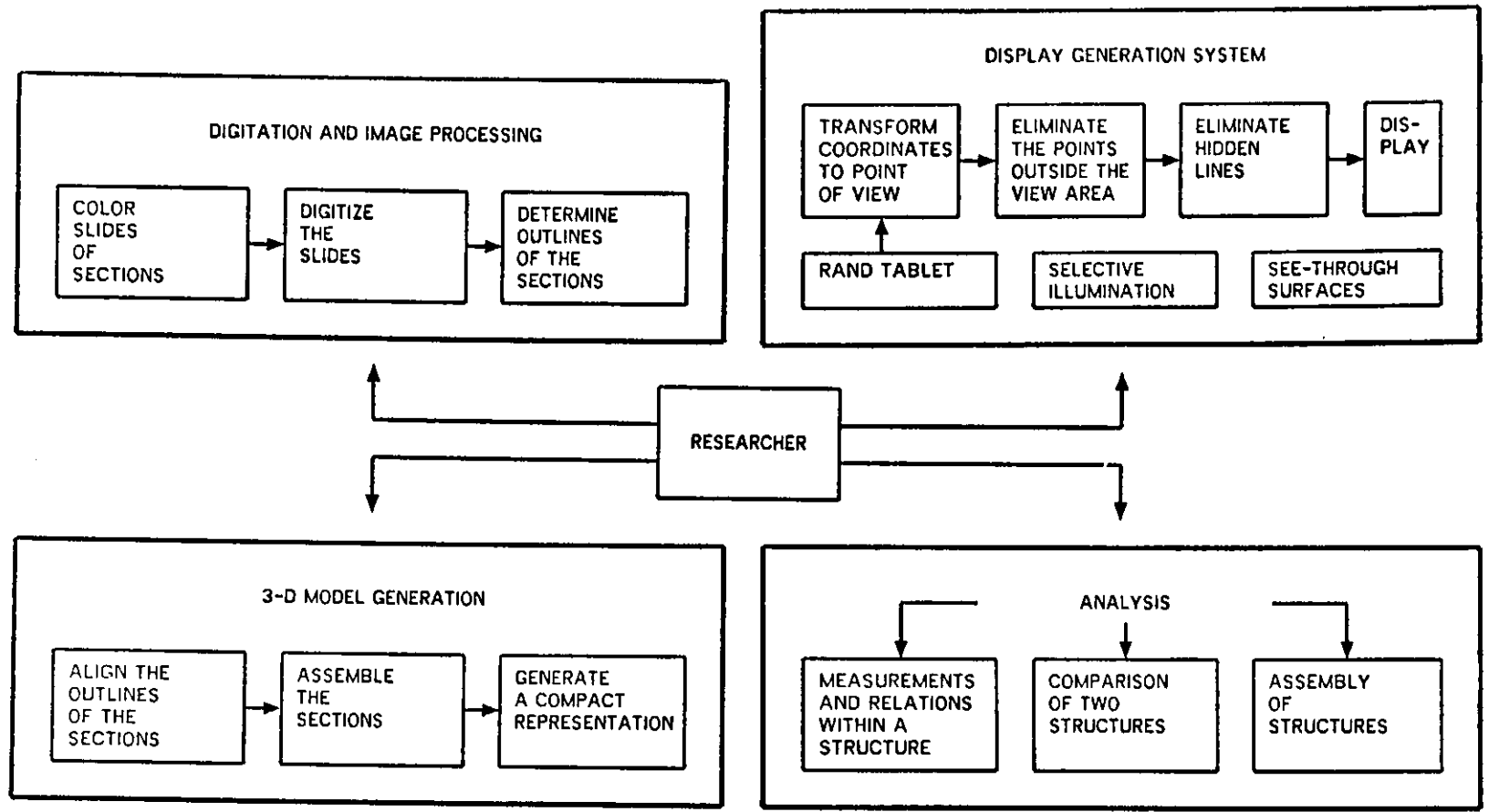


Figure 7-A. The programming sub-system (software) of the SYNAPS system.

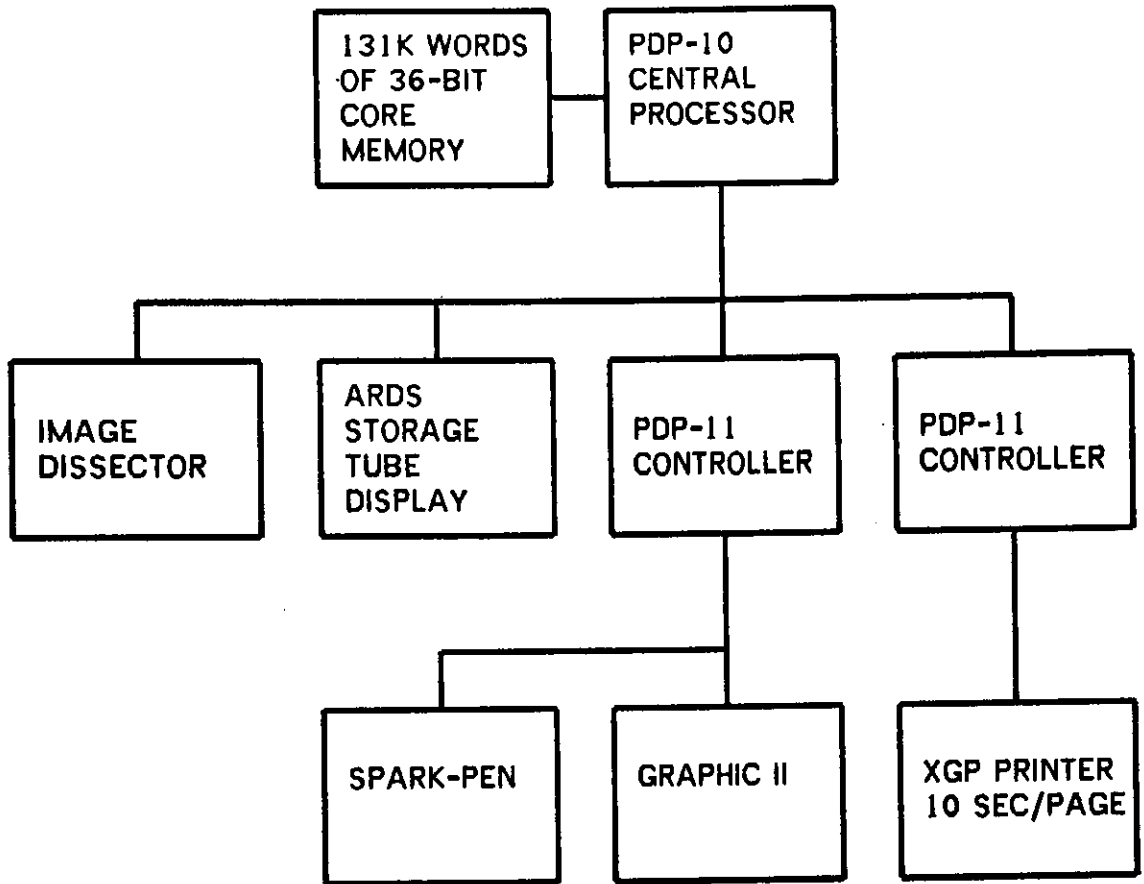


Figure 7-B. The computer sub-system (hardware) of the SYNAPS system. Conventional input-output devices such as card reader, line printer, magnetic tape etc. are not shown.

of a large PDP-10 computer (192K words of core storage), an image dissector, a Grafpen and tablet, a Graphic-II regenerative display system, a hard copy Xerox Graphic Printer, and a storage scope.

1. Input Devices

The image dissector (Information International, Inc.) is used to digitize 35mm color photographs of serial sections obtained from dye-injection experiments. A Kodak carousel projector with a special lens and filter projects the image from the photograph onto the photo-cathode of the image dissector (Fig. 8). The image dissector can be used to selectively digitize any point in its field of view, under program control. The outline of the image may also be traced manually using a Grafpen (Science Accessories 611). In this case the image from the serial sections is projected onto a tablet and traced by the experimenter using the pen (Fig. 9). The position of the pen is transmitted to the computer and displayed on a CRT to provide immediate feedback to the experimenter.

2. Output Devices

In order to view the three-dimensional neuronal structure from any desired angle, a display system capable of performing translations and rotations is required. We have several such devices available, each having unique capabilities. The choice is dictated by the particular needs of the experiment.

The storage scope (Tektronix 611) is used for long-term display of a complex, flicker-free image. The main disadvantages of this device are that it is relatively slow (2-3 minutes for drawing a typical nerve cell of 1000 small, straight-line segments) and modification of any portion of the image necessitates erasing and re-drawing the entire image.

The Graphic-II regenerative display (Bell et al. (1971)) is used for translation and rotation of the image in real time. In addition, selected portions of the image can be modified without re-drawing the entire image. To avoid "flicker" in the display, however, the complexity of the image is limited to one which can be generated in less than 30 msec.

The Xerox Graphic Printer (Reddy et al. (1972)), has the advantages and disadvantages of the storage scope, and in addition yields a permanent copy. Views from many different angles may be produced and examined together later "off-line". All the diagrams presented in this paper were produced using this device.

None of the above devices permit rotation of the complex structures in real time, with the attendant kinetic depth effects. The LDS1 graphics system (Evans-Sutherland Corporation), with its hardware matrix multiplier and clipping divider, displays complex, flicker-free images which can be rotated in real time. This system is expensive to purchase, but is available to us on a rental basis over a national computer network (ARPA network).

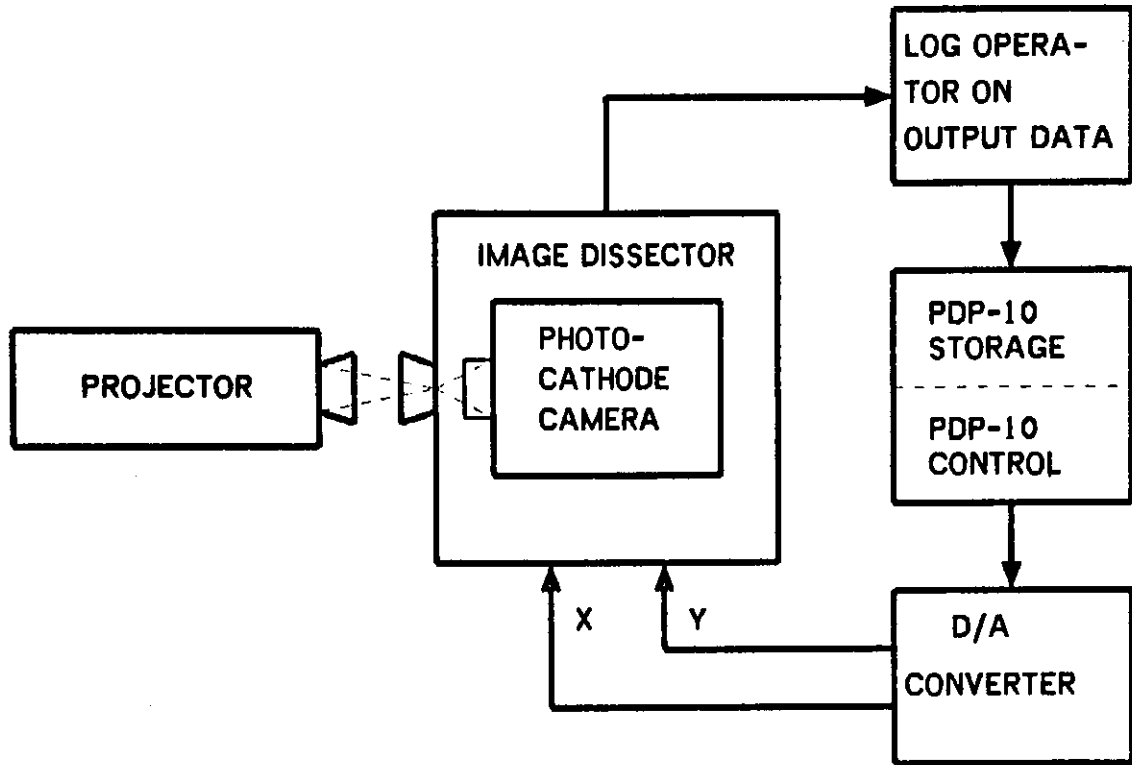


Figure 8. The Image Dissector. The X and Y coordinates of the point to be digitized are converted to analog inputs providing proportional currents to the deflection coils of the image dissector. The deflected electron beam from the selected point passes through a narrow aperture. Thus measuring light at a selected point on the photo cathode consists of integrating the signal which is proportional to the photo electrons emitted from the photo cathode. The time taken for the integrator to reach a particular threshold is measured. This time is inversely proportional to the average signal amplitude during the integrating period. The log value of this time is calculated and transmitted to the computer for subsequent image analysis.

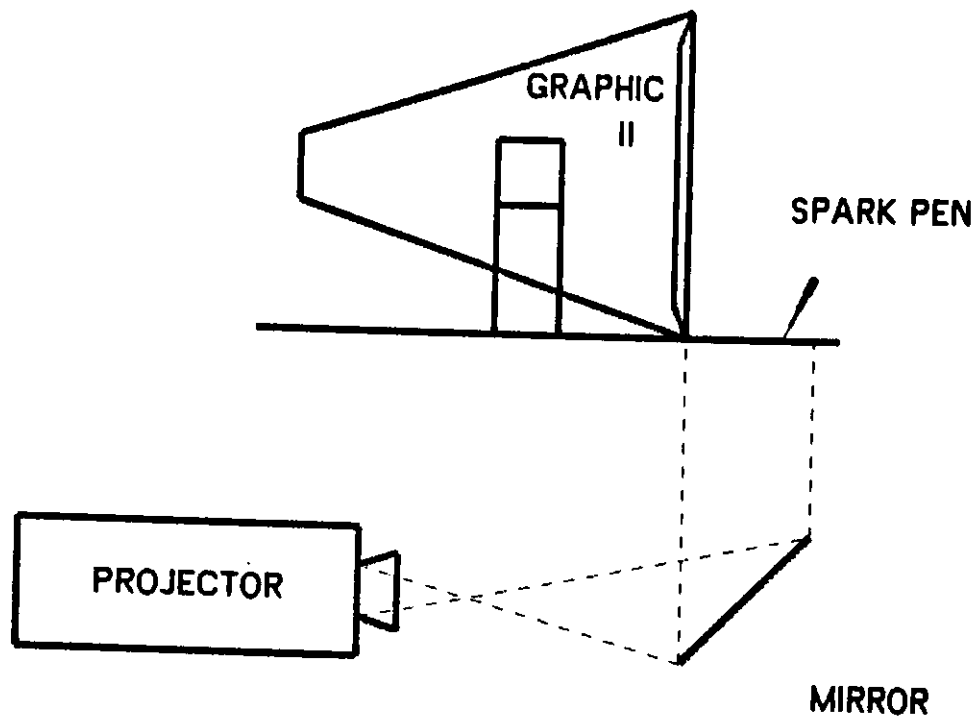


Figure 9. The Graf-Pen. The device is based on spark chamber technology. It consists of a stylus which has, at its tip, a repeating spark discharge. Each time a spark is generated a counter is started. Linear microphones placed along the X and Y axis are used to detect the arrival of the sound from the spark discharge. When the sound arrives the counter is stopped. The value of the count is proportional to the distance of the stylus from the microphone.

C. THE PROGRAMMING SYSTEM (SOFTWARE)

1. Digitization and Analysis of Sections

The purpose of digitization and analysis of images is to extract the relevant data from each section for use by the assembly program (see next section, Generation of the Three-Dimensional Model). The relevant information usually consists of the boundary of the ganglion, dendritic profiles, and other neuronal "landmarks". The boundary of the ganglion and other large structures are approximated by a series of straight lines, and internally represented as a list of lines. Smaller dendritic profiles are approximated by a circle, and internally represented by the center location and the radius of the circle. The relevant information can be extracted from the section either manually or automatically.

a. The Manual Method

In the manual method, the experimenter subjectively decides what information is relevant and traces the outline using the Graf-pen (Fig. 9). Every few milliseconds the location of the pen is transmitted to the computer. A line-fitting program operates on this coordinate data to fit a series of straight lines based on least square error criteria. The experimenter then manually types in whether the outline just traced is a ganglion boundary, a giant fiber or a dendritic profile. Data prepared in this form can now be used by the assembly program directly (see next section, Generation of the Three-Dimensional Model).

b. The Automatic Method

Tracing of the outlines by the experimenter is tedious and error-prone. Errors can result from incorrect tracing of data and from inaccurate judgments. The goal of the automatic method is to obtain dendritic profiles and other boundaries with minimal effort. This is achieved by the use of an "intelligent" image analysis program which operates on the digital representation of the slide from the image dissector (Fig. 8). The input to this program is a matrix of light values representing the original section, and the output from the program is the location and shape of the dendritic profiles and other landmarks. This approach raises several new problems. Some of these problems are associated with ensuring that the matrix of light values is a faithful representation of the original image, while others are related to image analysis.

Image digitization and associated problems. The first problem involves the preliminaries associated with the digitization process. The projected slide of a single section of a ganglion is positioned, illuminated and focussed with reference to the image dissector. Each of these preliminary steps is under program control. Proper illumination of the image, for example, is accomplished by a program which analyzes the entire range of light intensities from all digitized points in the projected image and recommends increasing or decreasing the lens aperture to obtain the maximum dynamic range. A focussing program scans the image, locates a boundary and recommends adjusting the focus of the projector to minimize blur (to maximize the rate change in digitized light intensities across the boundary). Following these steps, a digitization program scans the section to generate a matrix of light intensities (up to 1000 x 1000 points). To insure that the image is accurately digitized some form of

computer output of the image is required. Conventional output is woefully inadequate for such a purpose. We have developed several alternate output techniques over the last few years. Figure 10 shows several different forms of computer output of the digitized image of the photograph shown in figure 3.

The second problem in digitization arises from attempts at selective, high-resolution digitization of specific regions of a section. Such magnification may be desired by the user, or alternatively may be needed by the assembly program. Such a need may arise, for example, when a dendritic profile is absent where one is expected from information in adjacent sections, or when an apparent profile is present where one is not expected. Selective magnification can be achieved under computer control by an automatic pan, tilt and zoom mechanism. Such techniques are not yet available on our system but are under development. At present we manually perform the pan, tilt and zoom operations. Figure 11 shows a selective magnification of the marked area of the image digitized in figure 10.

The third problem in image digitization results from excessive demands on storage and bandwidth and cannot be performed conveniently on slower and smaller computers. The data obtained from a single dye injection experiment can generate more information than can be accommodated even by the larger billion-bit mass memories. For example, using the image dissector, a single section can result in 10^7 bits of data (1000 x 1000 matrix of light values with 10 bit accuracy per sample). If a single ganglion yields 250 sections one has to store and later process 2.5×10^9 bits of data. Assembling a composite neuronal network of only 10 neurons would involve 2.5×10^{10} bits of data! To ease this severe data storage requirement, we developed image compression programs which reduce the storage by an order of magnitude, using special encoding techniques. Both compression and subsequent re-expansion for further processing require special programs and necessitate an increase in computer processing time (so called time-space tradeoff).

Image analysis and associated problems. The image processing program operates on the raw data to locate the boundaries of the ganglion and dendritic profiles. This analysis is based on the fact that different regions of interest on the original slide are signified by discontinuities in light values in the digitized raw data. The discontinuities in the light values are located (and regions delimited) by an edge following program. This program uses a difference operator (analogous to differentiation) which indicates the direction and intensity of the discontinuity at a given point in the image. Low values of intensity indicate the absence of an edge. When an edge is present the direction of the discontinuity can be used to predict where the next point on the boundary of that region may be found. Figure 12A shows the results obtained after using a boundary detection operation. As shown in figure 12B, normalization of light values allows us to obtain a contrast enhancement of figure 12A. Figure 12C illustrates an attempt at edge detection by applying a difference operator. Note that many undesired regions appear in the output. By applying a thresholding operation to the subsection given in figure 11 we obtain the results of figure 12D. This operation involves ignoring all the variability in light values over a given threshold thereby eliminating undesired regions. Figure 12E shows the results of thresholding and edge detection on the subsection to locate dendritic profiles. Dendritic profiles obtained by thresholding and edge detection on the entire image is shown in figure 12F.

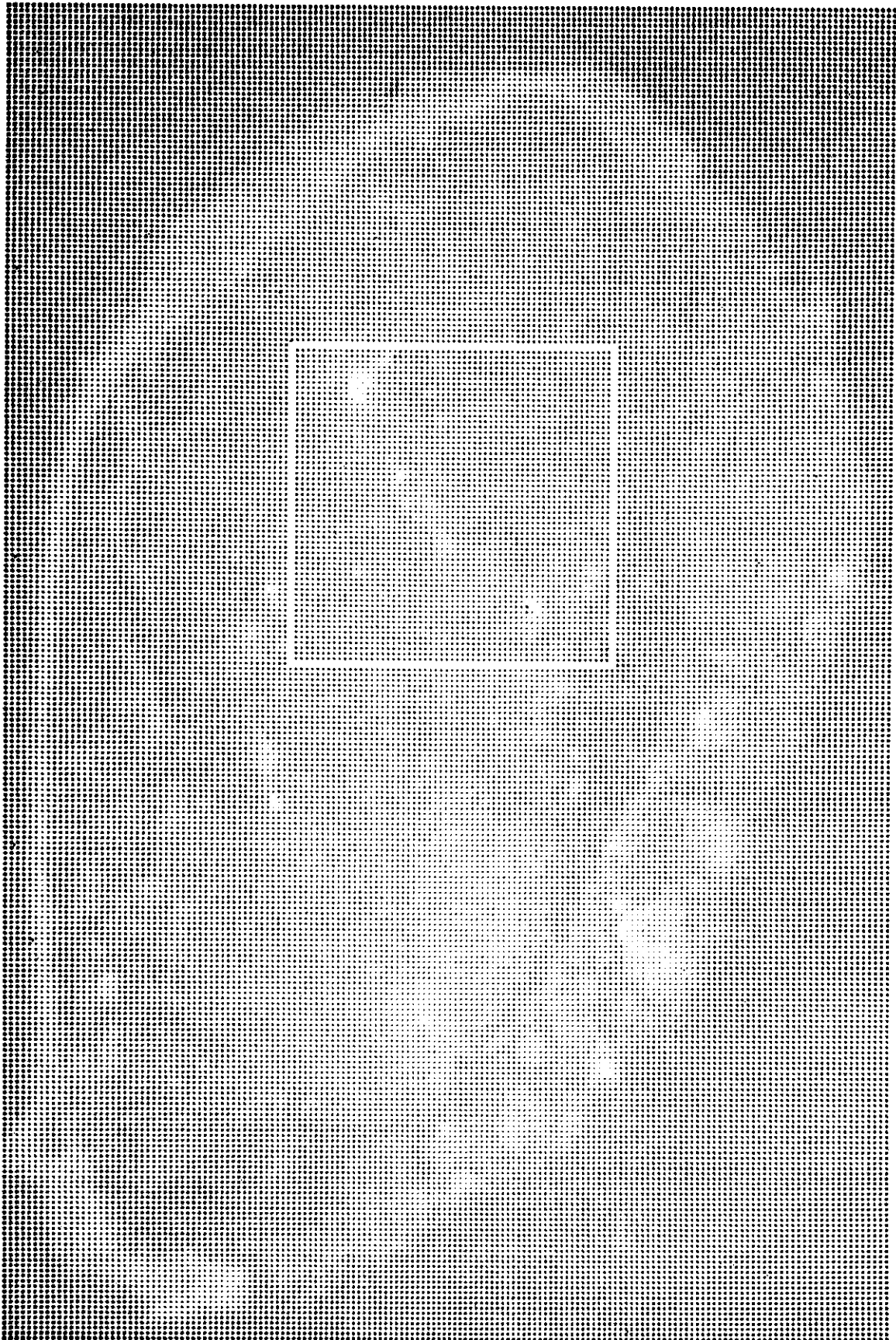


Figure 10-A. A digital reconstruction of the figure in 3 using the Xerox Graphic Printer; data is normalized to 16 levels of grey scale.

	1,	11,	21,	31,	41,	51,	61,	71,	81,	91,
1	FFFFFFFF	EEFF	ECCBBA7666	56765554322333	4666764355566565667666678788866677887777788877778886677766788889					
2	FFFFFFFF	EDBAAA9888	76654433211345	6665453344455676678765888787688877888788877777777777678888878						
3	DDDDDD	DECAAD8887	66544433222577	6431,11135667888777	77766899876789A87887678A988888788788787878					
4	EEEEEE	EEDCCA9A9875	34543244445766652,,256787776887666766656678987678899AAA97898788877888766						
5	FFFFFFFF	EEEDBBA88864	332345443334343,,126777667778876775545556789877789AA99AAR8888888988777777						
6	FFFFFFFF	FDUDBA767642	33337731,143232,,27998777766689877766668777898767AABA9ABA9888888988777787						
7	FFFFFFFF	FDCCCA866652	2234552,....,11,,1367887577876767766765655767776778AABBB8CBA977889888A767888						
8	FFFFFFFF	DDDCR986643	2236542,....,156678	8866677544577496765666877777789BDDCCB98899AA888777787						
9	FFFFFFFF	EDBBA8678865	77532,....,13566689	A8876445556663466777767787667899A8889988998777788						
10	FFFFFFFF	EDUDBA87632	357754,....,1355556A	988764455664335777887777777666689AA9A888888878888888						
11	FFFFFFFF	DDDBCA987769	44564541,....,3344566667	888865433336776678877777655889989889888888788						
12	FFFFFFFF	EDBBBA867886	5775532,....,24447754	8AAAABA61,344456667778985798556788777778887667787						
13	FFFFFFFF	DDBBBCA989888	99883221,....,24555567	789ABCBA73,234445688888765566654566556788776677778						
14	EEEEEE	EDDDCRA9AA88	9854322,....,1345545567	789ABBA9862112433566766677645656545665566787779867						
15	FEEDFE	EECBAAA8754	443321,....,2345578645	978877767776777675556678877777778887667788876678533						
16	EDDDCC	CCCCBA999A	8776553321,1,1,	124677875577866677789A86534543356656777558766655755456766778534						
17	EEDDCD	ERAA9ABBA98	877887676543224	211123675644334689876798766643225543456665668544665567677676534						
18	FDCDEE	CA9ARBA8976	7898877874145	3333345644333469AA88877545952,1,1343223977677675565456655677766664335						
19	FEDDED	RAAA9898876	7888889987433	44444454443555577789986954552,1,13344444777655677656676666776555556						
20	FFFFFF	EECCB999C999	888A98AAA87655	433355455555556677774414532113555434357655788667777667776676557						
21	FFFFFF	EDCBA9E98AAA	99A889AA97655	43564356555555556667535777578855666556678787666555567777878						
22	FFFFFF	EDDCAADA9AAA	99A888543564	456545435765445666677655788886556666543456578877534467788889A						
23	FFEDCD	DDCBA99A9BA	988888767543	2124544454324785445556655556788886556666765544568876545469AA998AAB						
24	FFEECD	BBDEEBA8AA	ACCA98887665	3333444543347844556654432345788876686767767555666666677A99AA8A8A						
25	FEDEED	CDDECRCA9AB	A988777697755	4344455444566533454232345788887666566566556666679A888A98						
26	DDBBBC	BBCCB888A8	7777776766544	4444433655554554344444456788997788888766666566566666676678ACDC98						
27	CCCCCB	BAABBB8A8	7656888778555	44555644334444556543444455667778888888778887664565656775579RCDB8						
28	DDCBBB	BBB8887798	8788845455344	467752,1,22356754444544445556678888887666754445654567765567789988						
29	DDCBBB	BBB8887765	544455676521,	1,2344575422341,1367777787878666655545545765567766677656						
30	DCBAAB	CCBCEFFFFF	EE87789A77644	44546776531,1,13455532441,1355546678876676554456555655576655435						
31	DDBBBC	DEE8887789	877898753445	566665542,1,2233334442242455556778A756656656654577555688764323						
32	DDDEEE	EECCEDCDDCA	AA8877887664	445677655653,1,1,2,34334322344457878A975568865446655677688888633						
33	DFEEDF	FEEDCRAA9A	888A9AA98877	65445776665543,1,1,25322333344422442244466889A8556876545545667788789866						
34	FFEEFF	FFFECDAB8A	8A8A8A8A8678	87878987656532123466644443345543356555678A9767899754456677677688CA7						
35	FECDDF	FFFD8A9ABBA	AAA9BAAAAA88	8889AA866544333344564542334444556556788AA76789887556664378888A8BA7						
36	FDDFFF	FFFC9A8BBBA	AA899ADDB98	88899666676443332344422343444334565455789877888887766655678889AAA8						
37	CDEEDEF	FEEDDB98A	8ABA9ACDA88	888787876777752,1,123322221122244445666656666777766665555666577777						
38	DEEDEF	FEEDB8A8E	DA989A8DCA9	99BBAAA98778877677642,1,13222,1,233334455555544444576456544455775566667						
39	EEEEEF	FB89ACFEED	CAAA8E888AA	ACC99888766777532,1,1,2221,1,133333345444464443457665544456787667888						
40	FFCCFF	FD8ABCDCDE	EEECBBE8887	7887788876543222222221,1,2334432355444556543468875446667788767887						
41	FDBACD	CBBDDBABCC	CBCCDEFFFB	BA989A98777778765454442,1,12221,12234333334444454333588755667655666777						
42	EA9ACB	9898DDB9A	9BC8BADEFF	EDBA99887766556556545542,1,12221223433333354433554457876667765447767						
43	98AD09	769A9CEDA	BAAAAAAACCE	DA998866566554455555667521123324443343345543454444666777876568987456777						
44	8ABBA9	898879ADE	DBAA8BBB8CB	A8986556665434455577876433433344443456559445676688866588AA988655677						
45	BB9889	8BDBA9ABRD	DOCA8BBB8C	CA88887656554324566556897645443332111234555554445556677778A8A88864455						
46	BB78AD	E8E8CDDDEE	FFDCDDDBA9	9AA9999A88875445786578A86643346763,1,1,234444454344565544567888888AA85435						
47	988ABC	DDCCCEFFFD	8BBBCEDBAAA	AA899A888787678A87642136763,1,1,2345322346564444345567678A886655						
48	9ACDFE	DDDDDFEFF	FE8BBBCDEE	B9ABA988999A8A888787668A8644445567631,1,1,344444334445432336659899AA88765						
49	0DFFFF	EEFFFFFEE	FE8A9A9999	888777666776667799A7764456665341,1,1,12454433223332333333344444444445556677756						
50	0EFFFF	FFFFFEEFF	E8CBBDA9AA	999887776655668865777778876666764432223344432223323454455788756665555						
51	FFFFFFFF	FFFFFFFFFE	CBABA88887	7877556577677654567799A866669333345322334443223322445556776555455565						
52	FFFFFFFF	FFFFFFFFF	FDABBA8788	7667754677665665667799ACA76754445454422233333333333444444444455555666						
53	FFFFFFFF	FFFFFFFFFE	BABA976787	54456545665455555579AAACB76777555665434433354422233333444445455666						
54	EEEEEE	FFFFFFFFFE	DBAAN77632	3567766676555555558A8897546666434555443333224444333443333445323454						
55	DDFFFF	FFFFFFFFFE	DEBA878774	113455647766665444555568A8556765533456455432222332233232123444432222						
56	EEFFFF	FFFFFFFFFE	DDDDCDBA7	76776544654676676664544565457886688765323564554333322222222,1,12334222212						
57	CCDFFF	FFFFFFFFFE	DDDDCDBA8	777766544456566656545455557899756765432244443334432222221,12122222111223						
58	AA8EFFF	FFFFFFFFFE	EDDDBCAA9	888877677645666677655555767875566545433343333333321221122333321,1222						
59	8ABFFF	FFFFFFFFFE	EDCCBAAA	8BBB8A897765666656766655444556666787543334433343233544422222334443321,1						

Figure 10-C. Hexadecimal output (values 0 to 15 are represented as ".", 1-9, A-F) on the line printer of actual light values of the subsection shown in figure 10B.

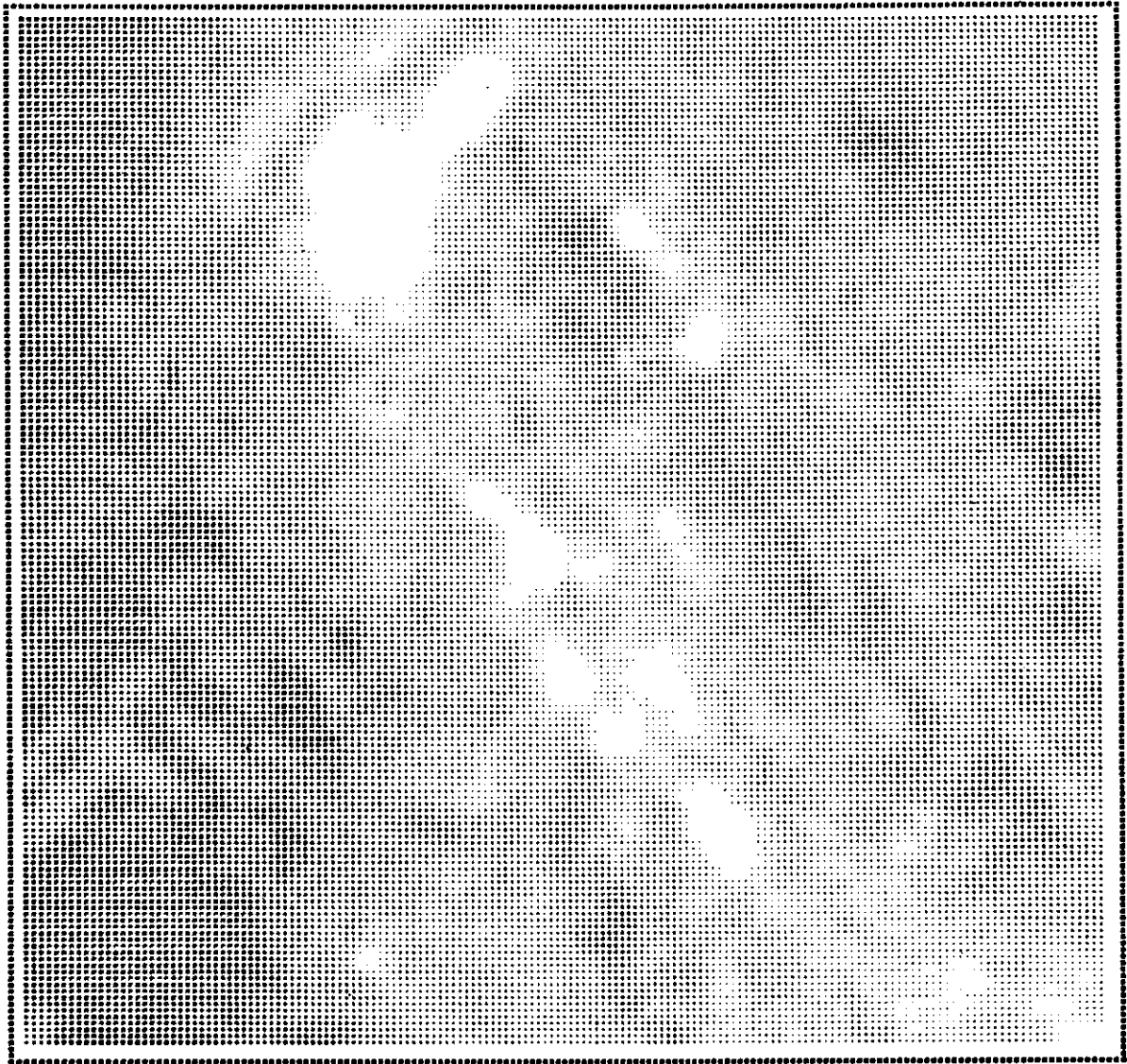


Figure 11. Selective magnification of the image delimited in figure 10A using the Xerox Graphic Printer. Note that several dendritic profiles missing in figure 10A are clearly visible in this magnified image.



Figure 12-A. Computer output after shell boundary detection operation on the original image.



Figure 12-B. Contrast enhancement operation on figure 12A through normalization of light values.



Figure 12-C. Attempt at edge detection of all interesting dendritic profiles and landmarks by applying a difference operator to the image in figure 10A; note that many undesired regions ("noise") also appearing the output.

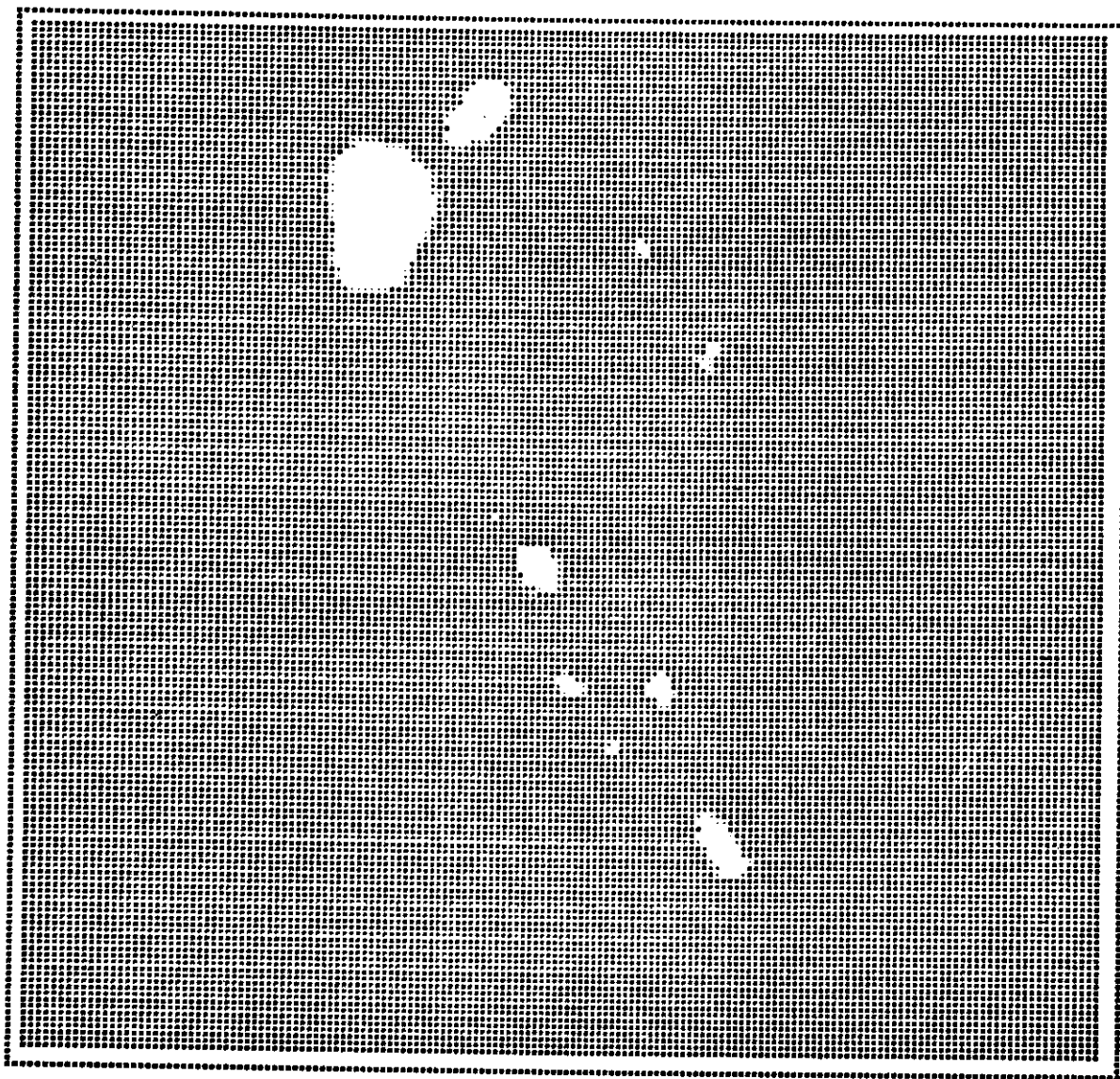


Figure 12-D. Elimination of some undesired regions by a threshold operation on the subsection given in figure 11, which involves ignoring all the variability in light values over a given threshold.

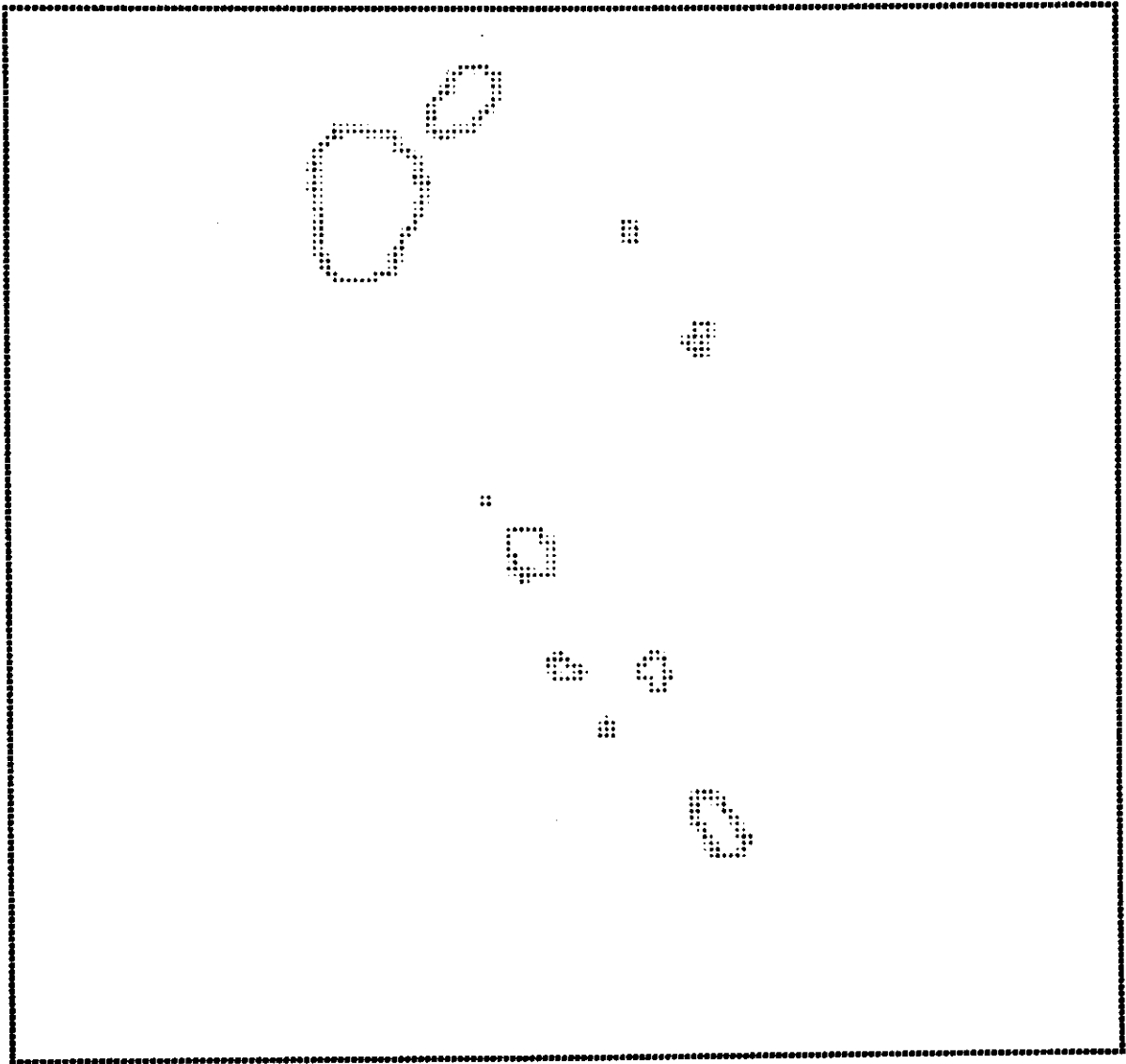


Figure 12-E. Thresholding and edge detection in the subsection to locate profiles.

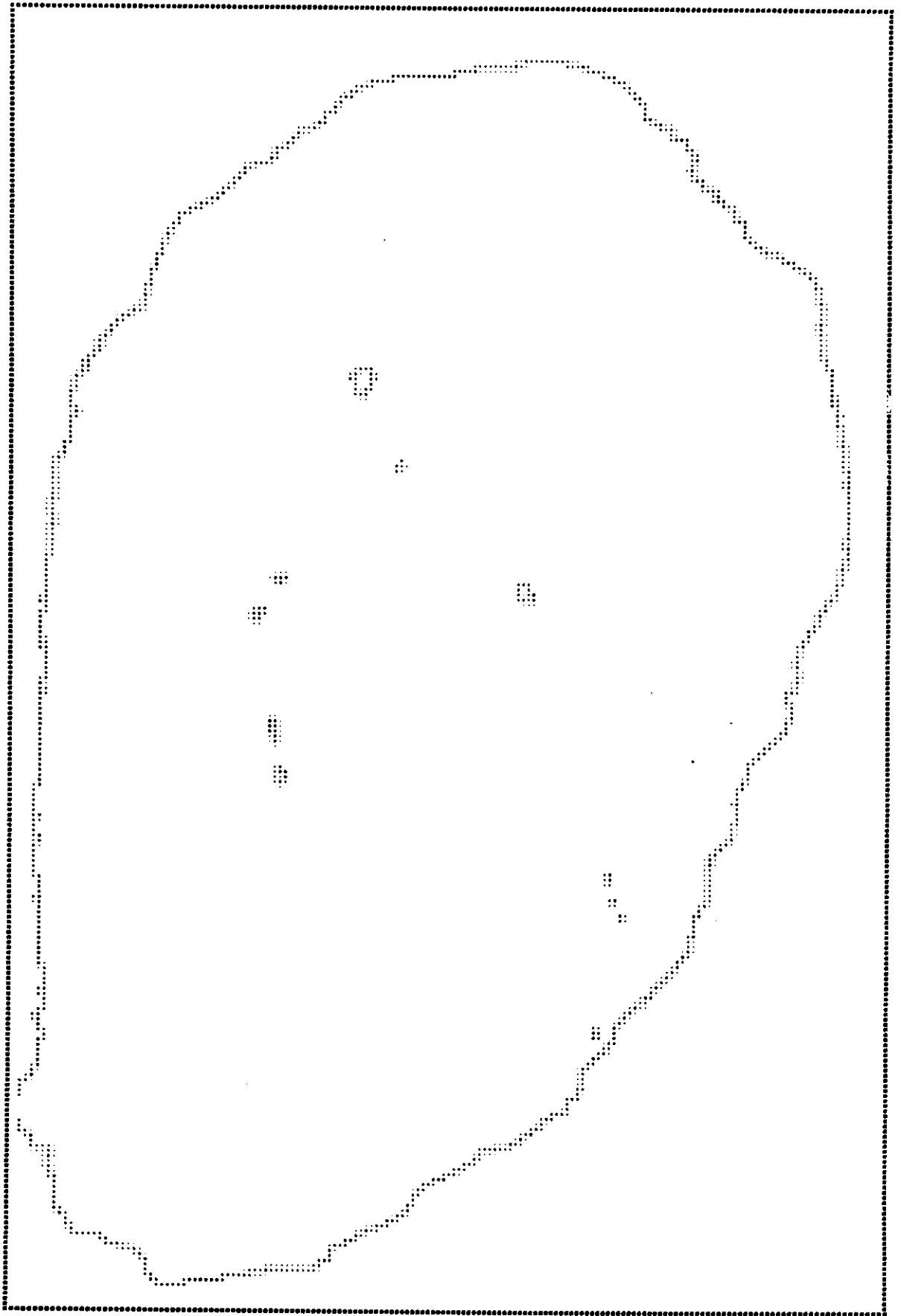


Figure 12-F. Dendritic profiles obtained by thresholding and edge detection on the entire image in figure 10A.

Although there is an increasing body of literature on image processing (Miller and Shaw (1968)); Rosenfeld (1969); Barlow *et al.* (1972)), analysis of naturally occurring scenes poses several previously unidentified and unsolved problems (Montanari and Reddy (1971)). The main difficulty is with noise which interferes with the analysis. Noise results from several sources: intensity differences caused by variable light transmission from one region to the next in a section, artifacts such as tissue or dust particles and unanticipated folds in the tissue, photographic distortions, uneven lighting of the microscopic field, undesired leakage of dye from the injected neuron, etc. This interference makes it necessary that the experimenter look at the results of image analysis and modify boundaries using the interactive image editor. Thus the automatic method is in reality a man-machine system with machine doing most of the work.

A variety of improvements in the above procedures are under development. Among the most important are programs which utilize information from adjacent sections for predictive purposes. The assumption that adjacent sections are more similar than different permits the programs to hypothesize regions where dendritic profiles may be found (thereby reducing processing time). Moreover, errors resulting from noise will be reduced by this procedure, since noise is unlikely to occur in corresponding regions of adjacent sections.

2. Generation of the Three-Dimensional Model

The boundary and profile information from the image analysis is assembled to form a single three-dimensional structure. This is achieved by combining a set of "line-lists" into a single, more complex data structure. In order to assemble the serial sections, a preliminary alignment operation is necessary owing to variations of the image position in the photographic field.

a. Alignment of Sections

The alignment of two adjacent sections requires the identification of at least two sets of corresponding points in both sections. This can be accomplished manually by visual observation of two superimposed outlines on a graphic display, or automatically by aligning corresponding landmarks in both sections by means of correlation procedures. The two sets of corresponding points are used to calculate a 2×2 rotation matrix and a translation vector, both of which define the amount by which one section must be moved to perfectly align the corresponding points. These transformations are then applied to all the points in the line-list of the section to be moved. This process is repeated between every pair of adjacent sections, resulting in a set of aligned sections.

The alignment described above only corrects for misalignments within the plane of the sections. Corrections to the coordinates are sometimes also required along the axis perpendicular to the plane. Although the serial sections through the ganglion are always parallel to each other, they may not be exactly perpendicular to the long axis of the ganglion. In such cases, the deviation from a precisely transverse angle is calculated from the information about the Z-axis (longitudinal) displacement between the anterior or dorsal margins of obvious, bilaterally-symmetric structures (the first nerve roots; identifiable daughter cells; etc). On this basis the necessary rotation of each section can be performed before assembly.

b. Assembly of Sections

Corresponding dendritic profiles in several adjacent sections are located and combined to form a single, straight line dendritic branch. This identification of the corresponding dendritic profiles is achieved by locating overlapping regions in adjacent sections. When a profile lacks an overlapping match in the preceding or following sections, a search is made to locate an unmatched profile in the immediate neighborhood. If no match is found the profile is discarded. Matched profiles are internally represented by variable-diameter, straight-line tubes. Profiles of small somata assembled from several sections are approximated by spheres. Profiles of large somata and the external surface of the ganglion are approximated by either triangular or irregular strip surfaces.

The result of the assembly operation is an internal data structure in which information about the dendritic structure is abstracted into a three-dimensional tree structure with all the branches located and identified, and with all linear proportions preserved. This representation is not only compact and concise, but it is also arranged in a form suitable for subsequent display and analysis.

3. Graphic Display of the Model

The graphic display provisions of the SYNAPS system permits the experimenter to view the reconstructed neuronal structure from different angles of view. This facility is not only necessary to inspect and modify the reconstruction but also to formulate intuitions about structural-functional relationships. The angle and position of view is specified by typing in the relevant values. We are at present designing a joystick-like analogue input which will permit the experimenter to "fly" through and around the neuronal structure to obtain different views of it. The effectiveness of the joystick increases when one is able to perform rotation in real-time.

A main problem in display generation is that we are dealing with non-mathematical surfaces and objects. An unselective display of all the subparts of the model usually results in a cluttered image (Fig. 13). Algorithms which generate transparent surfaces and/or eliminate hidden surfaces are available, but they are usually complex (Watkins (1970)) and cannot, at present, be implemented in real time without special-purpose hardware. One can simply eliminate the outer shell and other structures from the model (Fig. 14), but this results in the loss of crucial points of reference. Figure 15 illustrates our present compromise, i.e., elimination of giant fibers and use of a simple dotted-line representation of the shell, simulating a see through surface. The nerve structure may be displayed as straight lines (Fig. 15, A and B) or as tubes (Fig. 15C). Figure 16 shows the same neuron reconstructed in figure 15, but as viewed from several different angles.

Often the experimenter desires a close-up view of a subpart of a picture. SYNAPS is capable of giving a magnified, selective display of any portion of the neuron. Close-up views are much easier to provide using special purpose hardware such as the clipping divider (Sproull and Sutherland (1968)) available on the LDS1-graphic system.

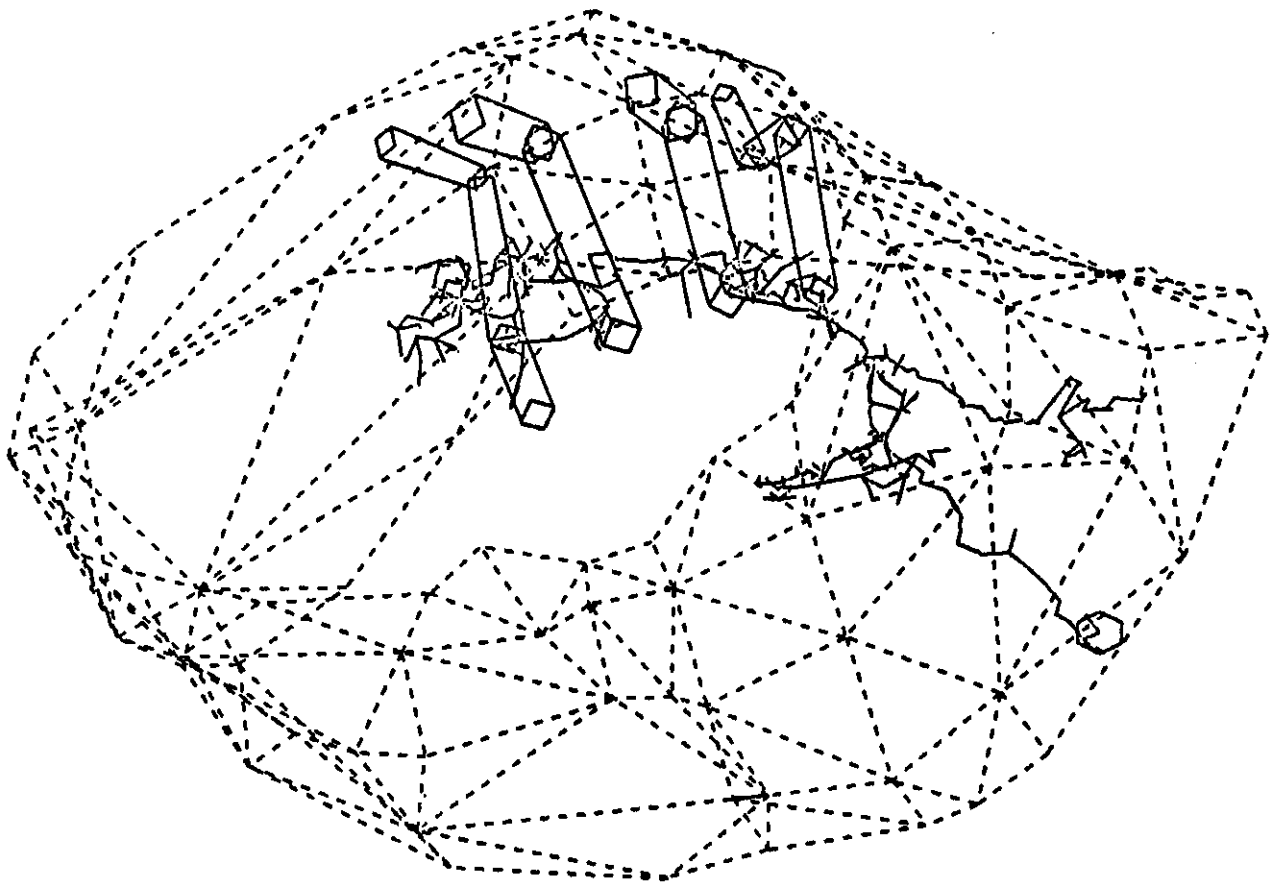


Figure 13. Cluttered image resulting from display of several subparts of the model.

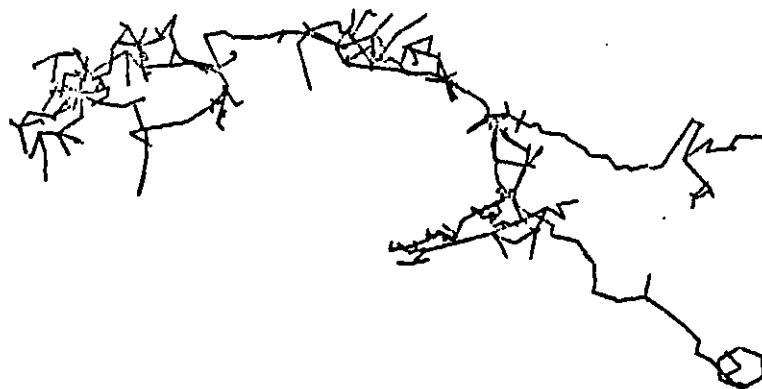


Figure 14. Display of the dendritic structure with the ganglion and giant fibers eliminated. This results in the loss of points of reference.

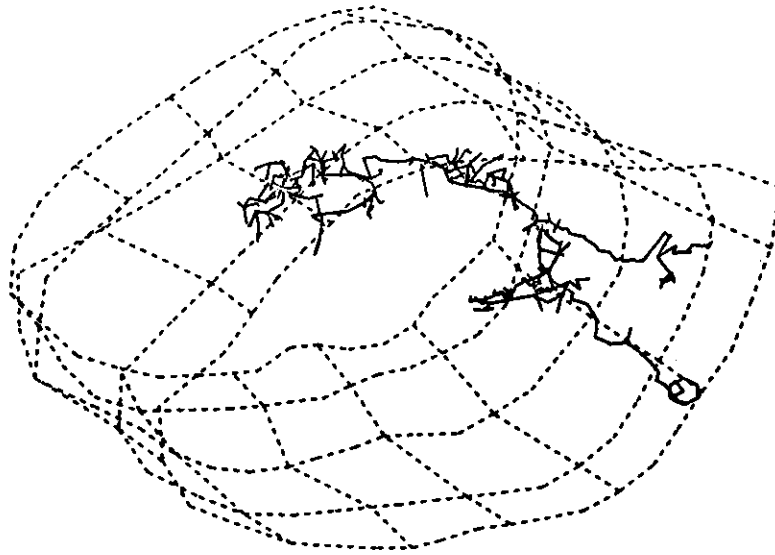


FIG. 15-A

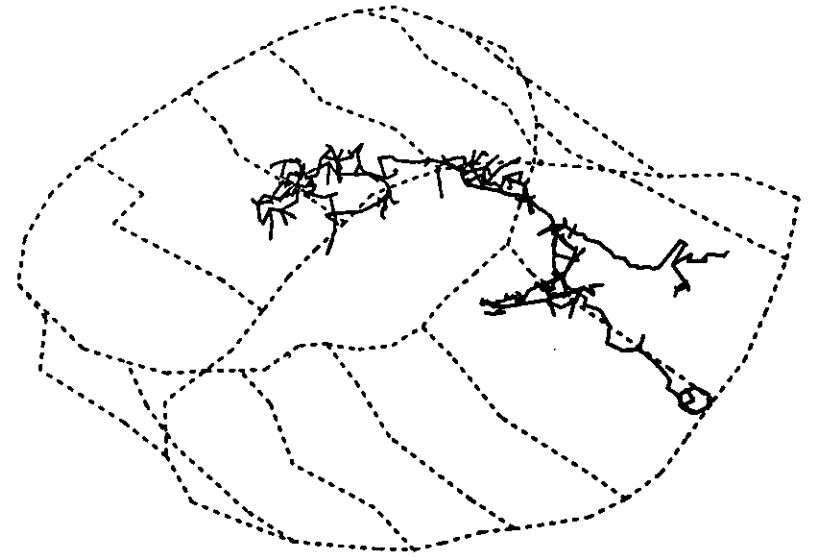


FIG. 15-B



FIG. 15-C

Figure 15. Different forms of display. A, shell represented by irregular patches with giant fibers eliminated. B, shell represented by strips. C, dendritic branches represented as variable diameter tubes.



FIG. 16-A

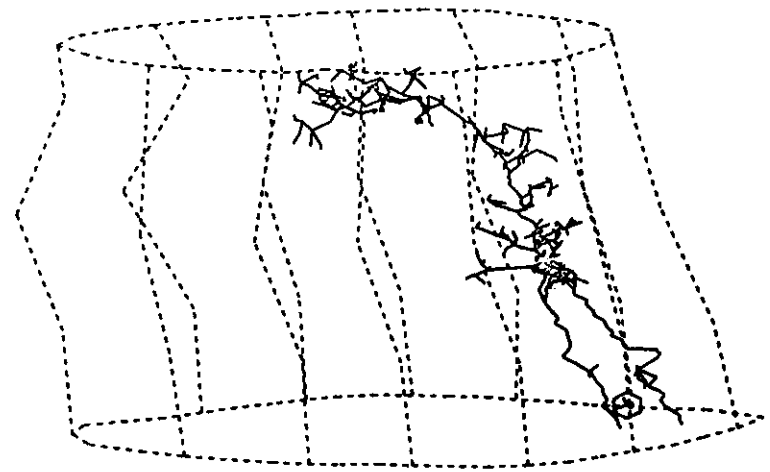


FIG. 16-B

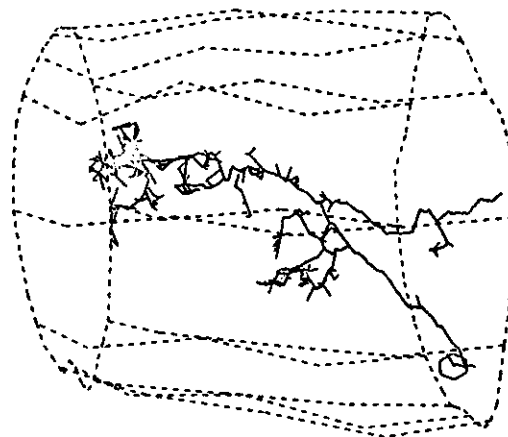


FIG. 16-C

Figure 16. Display of the model from different angles of view. A, Front view--angles of rotation about the x,y,z axes are 0,0,0. B, Topview--angles of rotation are 0,80,0. C, Side view--angles of rotation are 0,0,80 (x-axis out from paper, y-axis pointing right, and z-axis pointing upward).

4. Analysis of Reconstructed Neurons

Our eventual goal is to assemble a three-dimensional model of an architypical ganglion containing select, identified neurons. Postulated relationships between topological and functional properties of the reconstructed networks (Davis (1969)), if present, should appear especially conspicuous in such selective, composite reconstructions.

a. Qualitative Studies

The qualitative, three-dimensional reconstructions achieved to date (Figs. 15 and 16) are a necessary first step towards the above objective, and moreover they provide the basis for significant sub-studies. For example, with the computer techniques described above we can now qualitatively and accurately assess general morphological features such as the size and shape of dendritic fields. These features are in turn expected to bear interesting and testable relationships with the functional properties of the neurons (see Introduction).

Combination of several identified neurons into a single ganglion, on the other hand, presents somewhat more complex problems. For example, only one neuron is normally injected in each experiment to avoid ambiguities in the reconstruction. Therefore, data from different ganglia will have to be combined to obtain a topological map of a given network. Homologous ganglia appear qualitatively similar from one animal to the next, but significant quantitative differences in relative proportion may exist. In this case normalization of different ganglia may be necessary, and the required transformations may not be linear.

b. Quantitative Studies

As detailed in the Introduction, the development of a quantitative language for describing neuronal structure is an important eventual goal of this work. With the programs developed to date, we can extract the following quantitative data from single injected neurons: the number of dendritic branches, dendrite diameter, length, volume and, with reasonable simplifying assumption, surface area. These measures can be determined either for the entire dendritic field of a neuron, or for select regions of special interest. Additional parameters of interest include dendrite taper, branch pattern, overall shape and distribution, spatial position relative to other dendritic fields, and pattern of connection with other neurons. Some of these measures seem straight-forward and relevant to neuronal function, while others are only vaguely defined at present. In many instances we expect to have to resort to statistical descriptions, especially with regard to the shape of dendritic fields and their relative spatial positions. Many of the problems are clearly unforeseeable, and the solutions will simply have to evolve with the research.

SUMMARY AND CONCLUSIONS

This paper describes research to date on SYNAPS, (Symbolic Neuronal Analysis Programming System), a computer-based system for analysis of the the geometry of single nerve cells and the structure of neuronal networks. In its present, unfinished form, the system is useful only in the hands of trained computer scientists, and its capabilities are limited to: 1), acceptance of "edited" data on neuronal structure, consisting of tracings from serial sections of dye-filled branches of an injected neuron; 2), accurate reconstruction in three dimensions of the injected neuron and its surrounding ganglion; 3), rotation of the three-dimensional model so that the reconstructed neuron may be viewed from any angle and its spatial relationships with other structures qualitatively assessed; 4), selective, high-resolution display of desired regions of the injected neuron; and 5), extraction of quantitative data on the number of dendritic branches of an injected neuron, dendrite diameter, length, volume and surface area.

In its finished form, SYNAPS will be usable by biologists untrained in the computer sciences, for studying neuronal structure in any nervous system. Planned capabilities include: 1), automated input of "raw" data (although experience with intracellular dye injection suggests a need for extensive man-machine interaction); 2), quantitative description of the morphology of single neurons; and 3), quantitative analysis of the spatial relationships of many neurons in a network. Completion of SYNAPS will require solving numerous practical and theoretical problems in the computer sciences, but our experience to date suggests that a reasonably complete system can be implemented within five years. Completion of the system will open the way to rigorous studies of neuronal structure and its relations to neuronal function.

REFERENCES

1. Barlow, H.B., Narasimhan, R. and Rosenfeld, A. (1972). Visual pattern analysis in machines and animals. *Science* 177: 567-575.
2. Beurle, R.L. (1956). Properties of a mass of cells capable of regenerating pulses. *Phil. Trans. Roy. Soc. London B* 240: 55-94.
3. Bell, C. G., Reddy, D. R., Pierson, C. and Rosen, B. (1971). A high performance programmed remote display terminal. *Proc. of 1971 IEEE Computer Society Conf., Boston, Mass.*, 47-48.
4. Cohen, M.J. (1973). The form of nerve cells: Determination by cobalt impregnation. In: *Intracellular Staining in Neurobiology*. Editor, S.D. Kater and C. Nicholson. New York: Springer-Verlag.
5. Davis, W.J. (1969). The neural control of swimmeret beating in the lobster. *J. Exp. Biol.* 50: 99-117.
6. Davis, W.J. (1979). Motoneuron morphology and synaptic contacts: Determination by intracellular dye injection. *Science* 168: 1358-1360.
7. Davis, W.J. (1971). Functional significance of motoneuron size and soma position in swimmeret system of the lobster. *J. Neurophysiol.* 34: 274-288.
8. Fox, C.A. and Barnard, J.W. (1957). A Quantitative study of the Purkinje cell dendritic branchlets and their relation to afferent fibers. *J. Anat.* 91: 299-313.
9. Freeman, J.A. (1969). The cerebellum as a timing device: An experimental study in the frog. In: *Neurobiology of Cerebellar Evolution and Development*. Editor, R. Llinás. Chicago: American Medical Association, 397-420.
10. Globus, A. and Scheibel, A.B. (1967). Pattern and field in cortical structure: The rabbit. *J. Comp. Neurol.* 131: 155-172.
11. Henneman, E. (1957). Relation between size of neurons and their susceptibility to discharge. *Science* 126: 1345-1347.
12. Henneman, E., Somjen, G. and Carpenter, D.O. (1965). Excitability and inhibitability of motoneurons of different sizes. *J. Neurophysiol.* 28: 599-620.
13. Hilgard, E.R. (Editor) (1964). *Theories of Learning and Instruction*. Chicago: University of Chicago Press.
14. Hinkle, M. and Camhi, J.M. (1972). Locust motoneurons: Bursting activity correlated with axon diameter. *Science* 175: 553-556.
15. Hughes, G.M. and Wiersma, C.A.G. (1960). Neuronal pathways and synaptic connexions in the abdominal cord of the crayfish. *J. Exp. Biol.* 37: 291-307.

16. Kater, S., Davis, W.J. and Nicholson, C. (1973). A guide to intracellular staining techniques. In: Intracellular Staining in Neurobiology. Editor, S.D. Kater and C. Nicholson. New York: Springer-Verlag.
17. Kato, M., Fujimori, B. and Hirata, Y. (1968). An electron microscopic study of intracellularly stained neurons. *Brain Res.* 9: 390-393.
18. Kennedy, D., Selverston, A.I., and Remler, M.P. (1969). Analysis of restricted neural networks. *Science* 164: 1488-1496.
19. Kravitz, E.A. and Stretton, A.O.W. (1973). Intracellular staining techniques in neurobiology. In: Intracellular Staining in Neurobiology. Editor, S.D. Kater and C. Nicholson. New York: Springer-Verlag.
20. Ledley, R.S. (1964). High-speed automatic analysis of biomedical pictures. *Science* 146: 216-222.
21. Levinthal, C. and Ware, R. (1972). Three dimensional reconstruction from serial sections. *Nature* 236: 207-210.
22. Mannen, H. (1964). Arborizations dendritiques étude topographique et quantitative dans le noyau vestibulaire du chat. *Arch. Ital. Biol.* 103: 197-219.
23. Miller, W.F. and Shaw, A.C. (1968). Linguistic methods in picture processing: A survey, Proceedings of 1968 Fall Joint Computer Conference, 279-290.
24. Montanari, U. and Reddy, D. R. (1971). Computer processing of natural scenes: some unsolved problems. Proceedings of the AGARD Symposium on Artificial Intelligence, Rome.
25. Mulloney, B. (1973). Axonal iontophoresis of procion dyes and metals. In: Intracellular Staining in Neurobiology. Editor, S.D. Kater and C. Nicholson. New York: Springer-Verlag.
26. Murphey, R.K. (1973). Characterization of an insect neuron which cannot be visualized in situ. In: Intracellular Staining in Neurobiology. Editor, S.D. Kater and C. Nicholson. New York: Springer-Verlag.
27. Mungai, J.M. (1967). Dendritic patterns in the somatic sensory cortex of the cat. *J. Anat.* 101: 403-418.
28. Otsuka, M., Kravitz, E.A. and Potter, D.D. (1967). Physiological and chemical architecture of a lobster ganglion with particular reference to gamma-amino-butyrate and glutamate. *J. Neurophysiol.* 30: 725-752.
29. Pitman, R.M., Tweedle, C.D. and Cohen, M.J. (1972). Branching of central neurons: Intracellular cobalt injection for light and electron microscopy. *Science* 176: 412-414.
30. Pomeranz, B. and Chung, S.H. (1970). Dendritic-tree anatomy codes form vision physiology in tadpole retina. *Science* 170: 983-984.

31. Rall, W. (1967). Distinguishing theoretical synaptic potentials computed for different soma-dendritic distributions of synaptic inputs. *J. Neurophysiol.* 30: 1138-1168.
32. Rall, W., Burke, R.E., Smith, T.G., Nelson, P.G. and Frank, K. (1967). Dendritic location of synapses and possible mechanisms for the monosynaptic EPSP in motoneurons. *J. Neurophysiol.* 30: 1169-1193.
33. Rall, W. and Shepherd, G.M. (1968). Theoretical reconstruction of field potentials and dendrodendritic synaptic interactions in olfactory bulb. *J. Neurophysiol.* 31: 884-915.
34. Ramón-Moliner, E. (1962). An attempt at classifying nerve cells on the basis of their dendritic patterns. *J. Comp. Neurol.* 119: 211-227.
35. Ramón-Moliner, E. (1968). The morphology of dendrites. In: The Structure and Function of Nervous Tissue, vol. 1. Editor, G.H. Bourne. New York: Academic Press, 205-267.
36. Ramon y Cajal, S. (1911). Histologie du Système Nerveux de L'homme et des Vertébrés. 2 vol. Paris: Maloine.
37. Reddy, R., Broadley, B., Erman, L., Johnson, R., Newcomer, J., Robertson, G., and Wright, J. (1972). XCRIBL: a hardcopy scan line graphics system for document generation. Tech. Report, Carnegie-Mellon Univ., Pittsburgh. (Also to be published in *Information Letters*, 1973.)
36. Rosenfeld, A. (1969). Picture Processing by Computer, New York: Academic Press.
39. Selverston, A.I. (1973). Using dye injection to study the functional architecture of crustacean neurons. In: Intracellular Staining in Neurobiology. Editor, S.D. Kater and C. Nicholson. New York: Springer-Verlag.
40. Sproull, R.F. and Sutherland, I.E. (1968). A Clipping divider. *Proc. 1968 Fall Joint Computer Conf.* 33: 765-775.
41. Stretton, A.O.W. and Kravitz, E.A. (1968). Neuronal geometry: Determination with a technique of intracellular dye injection. *Science* 162: 132-134.
42. Thomas, R.C. and Wilson, V.J. (1966). Marking single neurons by staining with intracellular recording microelectrodes. *Science* 151: 1538-1539.
43. Verzeano, M. (1963). The synchronization of brain waves. *Acta. Neurol. Latinoamer.* 9: 297-307.
44. Verzeano, M. and Negishi, K. (1960). Neuronal activity in cortical and thalamic networks. *J. Gen. Physiol.* 43: 177-195.
45. Watkins, G.S. (1970). A real time visible surface algorithm. Computer Science Department, Univ. of Utah, UTECH-CSC-70-101.

46. Wiersma, C.A.G. and Hughes, G.M. (1961). On the functional anatomy of neuronal units in the abdominal cord of the crayfish, Procambarus clarkii (Girard). J. Comp. Neurol. 116: 209-228.
47. Woolsey, T.A., Wann, D.F., Cowan, W.M., Dierker, M.L. and Shinn C.M. (1972). Computer analysis of golgi impregnated neurons. Washington Univ., St. Louis, Presented at the Second Annual Meeting of the Society for Neuroscience, Houston, Texas.